Published in final edited form as:
Glia. 2010 March ; 58(4): 391–398. doi:10.1002/glia.20930.

ABSENCE OF OLIGODENDROGLIAL GLUCOSYLCERAMIDE SYNTHESIS DOES NOT RESULT IN CNS MYELIN ABNORMALITIES OR ALTER THE DYSMYELINATING PHENOTYPE OF CGT-DEFICIENT MICE

Laleh Saadat[1], **Jeffrey L. Dupree**[2], **John Kilkus**[3], **Xianlin Han**[4], **Maria Traka**[1], **Richard L. Proia**[5], **Glyn Dawson**[3], and **Brian Popko**[1]

[1]The Jack Miller Center for Peripheral Neuropathy, Department of Neurology, The University of Chicago

[2]Department of Anatomy and Neurobiology, Virginia Commonwealth University

[3]Department of Pediatrics, The University of Chicago

[4]Department of Internal Medicine, Washington University School of Medicine

[5]Genetics of Development and Disease Branch, National Institutes of Diabetes and Digestive and Kidney Diseases, National Institutes of Health

Abstract

To examine the function of glycosphingolipids (GSLs) in oligodendrocytes, the myelinating cells of the central nervous system (CNS), mice were generated that lack oligodendroglial expression of UDP-glucose ceramide glucosyltransferase (encoded by *Ugcg*). These mice (*Ugcg*$^{flox/flox}$*;Cnp/Cre*) did not show any apparent clinical phenotype, their total brain and myelin extracts had normal GSL content, including ganglioside composition, and myelin abnormalities were not detected in their CNS. These data indicate that the elimination of gangliosides from oligodendrocytes is not detrimental to myelination. These mice were also used to asses the potential compensatory effect of hydroxyl fatty acid glucosylceramide (HFA-GlcCer) accumulation in UDP-galactose:ceramide galactosyltransferase (encoded by *Cgt*, also known as *Ugt8a*) deficient mice. At postnatal day 18, the phenotypic characteristics of the *Ugcg*$^{flox/flox}$*;Cnp/Cre;Cgt*$^{-/-}$ mutants, including the degree of hypomyelination, were surprisingly similar to that of *Cgt*$^{-/-}$ mice, suggesting that the accumulation of HFA-GlcCer in *Cgt*$^{-/-}$ mice does not modify their phenotype. These studies demonstrate that abundant, structurally-intact myelin can form in the absence of glycolipids, which normally represent over 20% of the dry weight of myelin.

Introduction

Gangliosides are sialic-acid-containing GSLs, which are abundant components of neural cells and are present at high concentrations in axonal membranes and synaptic terminals (Eichberg et al. 1964). Additionally, two gangliosides, GM1 and GM4, have been found at low concentrations in rat and human myelin, respectively (Asou et al. 1985; Kotani et al. 1993; Ledeen et al. 1973; Suzuki 1970; Suzuki et al. 1968; Suzuki et al. 1967; Ueno et al. 1978). Although the function of gangliosides in neuronal cells has been extensively studied, their function in oligodendrocytes has not been fully investigated.

Address correspondence to: Brian Popko, 5841 South Maryland Avenue, MC2030, Chicago, IL 60637-2030. FAX 773 702 577; bpopko@uchicago.edu.

In one branch of the bifurcated GSL biosynthetic pathway, ceramide is converted to galactosylceramide (GalCer) by UDP-galactose:ceramide galactosyltransferase (Cgt), and then to either GM4 or sulfatide (Coetzee et al. 1998; Morell and Radin 1969; Schulte and Stoffel 1993; Stahl et al. 1994). Alternatively, ceramide can be converted to GlcCer by UDP-glucose:ceramide glucosyltransferase (Ugcg), which catalyzes the transfer of glucose from UDP-glucose to ceramide (Ichikawa et al. 1996; Morell and Radin 1969). More complex gangliosides with a GlcCer core are generated through the subsequent actions of GD3 synthase (encoded by *Siat9*, also known as *St3gal5)* and GM2/GD2 synthase (encoded by *Galgt1*, also known as *B4galnt1*), which are responsible for GM3 and GM2 synthesis, respectively (Kolter et al. 2002; Yamashita et al. 2005b) (Fig. 1A).

Previous studies have assessed the significance of gangliosides in the CNS by disrupting the genes encoding different glycosyltransferase enzymes in the ganglioside biosynthesis pathway. Ceramide is the first substrate in ganglioside biosynthesis. Inactivation of *Ugcg* results in embryonic lethality (Yamashita et al. 1999). Deletion of *Galgt1* results in animals that are unable to synthesize GM2, GD2, GM1, GD1a, GD1b, and GT1b, and display axonal degeneration and dysmyelination of the optic nerve (Sheikh et al. 1999). Loss of both *Galgt1* and *Siat 9*, which results in the complete absence of GlcCer-based gangliosides, leads to a shortened lifespan, perturbed axo-glial interactions, and abnormal paranodal domains (Yamashita et al. 2005b). Although $Siat\ 9^{-/-}$;$Galgt1^{-/-}$ mice demonstrate normal oligodendrocyte development, they are characterized by white matter vacuolization, as well as oligodendrocyte abnormalities (Yamashita et al. 2005b). Nevertheless, it remains unclear whether the observed affects result from the impairment of ganglioside biosynthesis in neurons or oligodendrocytes.

Mice lacking the ability to synthesize GlcCer in neuronal cells were generated by taking advantage of a conditional, “floxed” Ugcg allele (Yamashita et al. 2005a) in combination with nestin/Cre mice (Jennemann et al. 2005). Nestin is an intermediate filament protein that is expressed in neural stem cells, as well as peripheral nerves and muscle (Zimmerman et al. 1994). $Ugcg^{Null/flox}$;*Nes/Cre* mice appear normal at birth but display a dramatically reduced lifespan, ataxia, and neuropathy with peripheral myelin splitting. Additionally, $Ugcg^{Null/flox}$;*Nes/Cre* mice possess abnormal Purkinge cells and hippocampal neurons, suggesting an important role for ganglioside biosynthesis in neuronal maturation and function (Jennemann et al. 2005; Yamashita et al. 2005a). Nevertheless, since the nestin/Cre line used to generate these mice drives Cre expression in neuronal precursor cells, it is not possible to eliminate a glial cell contribution to the described phenotype.

The importance of the *Cgt* pathway in CNS myelination has been established (Coetzee et al. 1998). $Cgt^{-/-}$ mice display tremors, ataxia and a severely reduced lifespan. Surprisingly, these mice produce abundant compact CNS and peripheral nerve myelin, despite the inability to synthesize the myelin galactolipids (Coetzee et al. 1996; Dupree et al. 1998), which normally represent a considerable fraction of the dry weight of myelin (Coetzee et al. 1998). Myelin from these mutant animals contains hydroxyl fatty acid (HFA) GlcCer, which is not normally found in the CNS, indicating that *Cgt* deficiency results in the use of α hydroxyl ceramide in the *Ugcg* pathway rather than in the *Cgt* pathway, which normally converts it to HFA-GalCer (Coetzee et al. 1996; Dupree et al. 1998). The GlcCer that accumulates in $Cgt^{-/-}$ myelin is believed to partially compensate for the absence of the galactolipids (Coetzee et al. 1996; Coetzee et al. 1998; Suzuki et al. 1999) .

Because previous studies did not distinguish between neuronal and oligodendroglial effects, the first goal of the present study was to assess the importance of oligodendroglial ganglioside biosynthesis in myelination. These efforts utilized the Cnp/Cre transgene product to delete the floxed *Ugcg* gene in myelinating cells (Lappe-Siefke et al. 2003;

Yamashita et al. 2005a). In the second part of this study, we investigated the extent to which HFA-GlcCer accumulation in *Cgt*$^{-/-}$ myelin compensates for the absence of galactolipids by generating *Ugcg*$^{flox/flox}$*;Cnp/Cre;Cgt*$^{-/-}$ mice that lack both galactolipids and HFA-GlcCer.

Materials and methods

Mice

To eliminate the *Ugcg* pathway specifically in myelinating cells, floxed *Ugcg* mice (Yamashita et al. 2005a) were crossed with mice in which the gene encoding the Cre recombinase has been embedded into the gene encoding the myelin-associated enzyme 2', 3' cyclic nucleotide 3' phosphodiesterase (*CNP/Cre mice*) (Lappe-Siefke et al. 2003). Homozygous *Ugcg* animals were obtained by crossing *Ugcg*$^{flox/+}$*;Cnp/Cre* mice to *Ugcg*$^{flox/+}$ animals . To generate *Ugcg*$^{flox/flox}$*;Cnp/Cre;Cgt*$^{-/-}$ mice, *Ugcg*$^{flox/flox}$*;Cnp/Cre* and *Cgt*$^{+/-}$ mice were bred to obtain *Ugcg*$^{flox/+}$*;Cnp/Cre;Cgt*$^{+/-}$ mice, which were then interbred to obtain the mutant *Ugcg*$^{flox/flox}$*;Cnp/Cre;Cgt*$^{-/-}$ mice.

Genotyping

Mice were genotyped for the presence of the *Ugcg*^{flox}, *Cgt* null and Cnp/Cre alleles using tail genomic DNA. Primer 1 (5'- ATGTGCTAGATCAGGCAGGAGGGCTCATAG-3') and primer 2 (5'-CCAACAGATATTGAATGCGAATGCTCTGCC -3') were used to identify the *Ugcg* allele with a product size of 200 bp for wild-type and 250 bp for the floxed allele. Recombination was detected by PCR of genomic DNA using primers 1 and 3 (5'-GAGCCAGTCCATTACTCTCGTTGATTGCAT-3') as described (Yamashita et al. 2005a) (Fig. 1B). Two sets of primers were used to identify wild-type and *Cgt*$^{-/-}$ mice. The primers 5'-CTCTCAGAAGGCAGAGACATTGCC-3' and 5'-CATCCATAGGCTGGACCCATGAAC-3' amplify the wild-type allele; the primers 5'-TCGCCTTCTTGACGAGTTCTTCTGAG-3' and 5'-ATCATCATTGTGCCGCCAATTATG-3' amplify the mutant *Cgt* allele (14). Amplification of the Cnp/Cre transgene was performed as described (Lappe-Siefke et al. 2003).

Lipid Analysis

Total lipids were extracted from half brains of wild-type and *Ugcg*$^{flox/flox}$*;Cnp/Cre* postnatal day (PND) 18 mice by homogenization in 3 mL of PBS. Lipids were extracted by adding methanol (5 mL) and incubating at room temperature for 1 hr, followed by the addition of chloroform (10 mL). The upper phase was collected and the lower phase washed three times with an equal amount of theoretical upper phase (TUP) methanol:water:chloroform (48:47:3). The three TUP washes were pooled with the original upper phase, evaporated to dryness, resuspended in 200 μL water, and sonicated. Chloroform:methanol (6 mL, 2:1 v/v) was added, then the sample was vortexed and evaporated to dryness with nitrogen. This step was repeated several times to remove hydrophobic proteins. Gangliosides were resolved on Whatmann high performance thin layer chromatography (HPTLC) plates (10 cm × 10 cm LHP-K TLC plates) by two sequential developments in chloroform:methanol:0.25% KCl (50:40:10) followed by charring with 10% $CuSO_4$-8% H_2SO_4.

The lower phase was evaporated to dryness under nitrogen and subjected to alkaline methanolysis to remove phosphoglycerides (1mL of 0.6N NaOH for 1 hr). Following neutralization with 70 μL of concentrated HCl, salts were pelleted. $CHCl_3$ (2 mL) and water (0.6 mL) were added to the supernatant. The upper phase was removed and the lower phase washed with an equal amount of TUP to remove salt. The lower phase was evaporated to dryness. The extracted lipids were applied to HPTLC plates and developed in

chloroform:methanol:glacial acetic acid:water (70:25:8.8:4.5 v/v). Ceramide, hexosylceramides, and sphingomyelin were visualized by charring (Kilkus et al. 2003; Wiesner et al. 1997).

Mass spectrometric analysis of lipids

Lipid extracts were prepared as described (Cheng et al. 2007). Each extract was reconstituted with a volume of 500 μl/mg of protein in 1:1 chloroform/methanol, flushed with nitrogen, capped and stored at −20 °C. Shotgun lipidomics analyses were performed as described (Cheng et al. 2007; Han and Gross 2005). The diluted lipid extract solution was infused directly into the electrospray ionization source with an automated nanospray apparatus (Nanomate HD, Advion Bioscience Ltd., Ithaca, NY) as described (Han et al. 2008). Data processing of shotgun lipidomics analyses including ion peak selection, baseline correction, data transfer, peak intensity comparison, ^{13}C de-isotoping, and quantitation were conducted as described (Yang et al. 2009).

Myelin Isolation

Myelin samples were isolated from PND 18 mouse brains by a modified Norton and Poduslo protocol (Norton and Poduslo 1973). Brains were homogenized in 2.5 mL of 0.32 M sucrose containing Tris-HCl buffer and overlaid onto 2.5 mL of 0.85 M sucrose. Samples were centrifuged using a SW50 rotor at 75,000 × g for 30 min at 4°C. The crude myelin membrane was collected from the 0.3/0.8 M sucrose interphase, resuspended with Tris-HCl buffer, pH 7.2, and centrifuged at low speed (12,000 × g) at 4°C to remove cytoplasmic and microsomal contaminants. Myelin was further purified by a second repetition of the density gradient centrifugation, followed by two cycles of 20 mM Tris-HCl, pH 7.4 washes. The final pellet was dissolved in 400 μL of 20mM Tris, pH 7.4.

Western blot

Brains were homogenized in lysis buffer that included 50 mM Tris-HCL, pH 7.2, 1% SDS, 1 mM PMSF, 5mM EDTA and 2 μg/mL of aprotinin. Samples were centrifuged at 14470 × g for 10 minutes at 4°C and protein concentration was measured using the Bradford Assay (Bio-Rad, Hercules, CA). 30 μg of protein were run on a 4–20% SDS–PAGE gel and transferred to a nitrocellose membrane. The nitrocellulose membrane was blocked by Tris Buffered Saline Tween-20 (TBST) containing 5% milk powder at room temperature, then incubated with individual primary antibodies at 4°C overnight. Primary antibodies were mouse anti-MBP (1:2000 dilution, Covance, Berkeley, California) and mouse anti-actin (1:1000 dilution, Sigma, Saint Louis, Missouri), and the secondary antibody was peroxidase-conjugated goat anti-mouse antibody (dilutions ranging from 1:3000 to 1:5000, Santa Cruz Biotechnology, Santa Cruz, CA). Immunoreactivity was detected using the enhanced chemiluminescence (ECL) reagent (Amersham Pharmacia, Freiburg, Germany). The ImageJ program was used to quantitate protein expression.

Histological Analysis

Animals were perfused with 4% paraformaldehyde and 2.5% glutaraldehyde in 0.1 M sodium phosphate buffer. Cervical segments of spinal cords were dissected, postfixed in perfusion buffer for one week, and processed for embedding in epon. Ultrathin sections of 60-90 nm thickness were stained with uranyl acetate-lead citrate and examined on a TEM microscope (JEOL, model JEM 1230 equipped with Gatan Ultra Scan 4000sp 4k X4K CCD camera). Morphometric analysis of myelinated fibers was performed on randomly selected EM fields from ventral spinal cord at a magnification of 5000X. Three to seven mice were used for each genotype. The G ratio for each mouse was calculated for a minimum of 100 myelinated axons per animal using NIH Image J.

Statistical Analysis

Results are presented as the mean ± standard deviation of three to seven mice per genotype. Mutant and wild-type values were compared by a two-tailed Student's t-test and differences were considered statistically significant if $P < 0.05$.

Results

Oligodendroglial *Ugcg* deletion does not alter brain ganglioside content

To determine the function of ganglioside biosynthesis in the myelination process, we crossed mice carrying a conditional allele of the *Ugcg* gene with Cnp/Cre transgenic mice, which express the Cre recombinase in oligodendrocytes (Lappe-Siefke et al. 2003). Deletion of the floxed *Ugcg* allele in the CNS of *Ugcg*$^{flox/flox}$*;Cnp/Cre* mice was confirmed by PCR analysis of genomic DNA from brain and spinal cord using the 1 and 3 primers, which specifically amplify the recombined allele (Fig. 1B). The 250 bp recombination product was clearly amplified from brain and spinal cord DNA, but barely detectable when amplified from heart DNA (Fig. 1C). The elimination of the floxed *Ugcg* allele was also confirmed by the absence of HFA-GlcCer in *Ugcg*$^{flox/flox}$*;Cnp/Cre;Cgt*$^{-/-}$ double mutants, as will be described in greater detail below.

The elimination of *Ugcg* expression in oligodendrocytes did not detectably affect ganglioside biosynthesis in the CNS (Fig. 2A). Total brain lipid extracts from PND 18 wild-type and *Ugcg*$^{flox/flox}$*;Cnp/Cre* mice were analyzed by HPTLC and all GlcCer-based gangliosides, including GM1, GD1a, GD1b, and GT1b, were found to be present in the mutant tissue at levels similar to those present in wild-type. To further assess the oligodendroglial contribution to ganglioside synthesis, we extracted myelin from PND 18 *Ugcg*$^{flox/flox}$*;Cnp/Cre* mice and wild-type littermates and examined the ganglioside content. The ganglioside patterns of both genotypes were identical. Small amounts of GM1, GD1a, GD1b, and GT1b were seen in both the wild-type and *Ugcg*$^{flox/flox}$*;Cnp/Cre* myelin (Fig. 2B). Because these gangliosides cannot be synthesized in the absence of *Ugcg*, their presence in the mutant myelin may be the result of neuronal membranes that are adhered to myelin, demonstrating that the myelin extraction procedure does not completely eliminate synaptic or axonal membranes, resulting in neuronally-derived membranes in the myelin samples. Alternatively, gangliosides in the myelin of wild-type and *Ugcg*$^{flox/flox}$*;Cnp/Cre* mice could have been acquired from other CNS cells or serum lipoprotein donors (Loeb and Dawson 1982;Senn et al. 1989;Shen et al. 1981). HFA and nonhydroxylated (NFA) GalCer and sulfatides were also detected in the neutral fractions of total brain (Fig. 2C) and myelin lipid extracts (Fig. 2D). NFA-GlcCer was not detected in the myelin of *Ugcg*$^{flox/flox}$*;Cnp/Cre* mice (Fig 2D).

Despite lacking *Ugcg* in oligodendrocytes, *Ugcg*$^{flox/flox}$*;Cnp/Cre* mice did not exhibit any abnormal clinical phenotypes during one and a half years of observation. Western blotting of total brain extract was used to monitor MBP expression and determine whether the elimination of *Ugcg* affects myelin production. Expression levels of MBP were similar in wild-type and mutants at PND 18 (Fig. 3A). Morphologically, myelinated axons from the *Ugcg*$^{flox/flox}$*;Cnp/Cre* animals were indistinguishable from wild-type (Fig. 3B and C). Furthermore, measurement of G ratios (axonal diameter/fiber diameter) in the ventral spinal cord revealed no differences between wild-type and mutant mice (Table 1). Additionally, detailed EM analysis demonstrated no difference in the percentage of uncompacted myelin sheaths in the mutants.

HFA-GlcCer is absent from *Ugcg*$^{flox/flox}$;*Cnp/Cre;Cgt*$^{-/-}$ mice

As previously described, NFA and HFA-GalCer lipids are not present in the CNS of *Cgt*$^{-/-}$ mice, while HFA-GlcCer accumulates in the mutant myelin (Fig. 4A). To determine if the HFA-GlcCer that accumulates in *Cgt*$^{-/-}$ myelin compensates for the absence of galactolipids, we generated *Ugcg*$^{flox/flox}$;*Cnp/Cre;Cgt*$^{-/-}$ mice. Lipid analysis of total brain and myelin extracts was performed on PND 18 *Ugcg*$^{flox/flox}$;*Cnp/Cre;Cgt*$^{-/-}$ mice to confirm the elimination of the HFA-GlcCer lipid. The disruption of *Ugcg* in *Cgt* deficient oligodendrocytes resulted in the complete disappearance of the HFA-GlcCer band in *Ugcg*$^{flox/flox}$;*Cnp/Cre;Cgt*$^{-/-}$ mice (Fig. 4A and B), confirming that the Cnp/Cre recombination system completely abolishes *Ugcg* enzymatic function in oligodendrocytes.

Ceramide levels were increased in the *Cgt*−/− and *Ugcg*$^{flox/flox}$;*Cnp/Cre;Cgt*$^{-/-}$ mice compared to wild-type mice (Fig 4B), which is consistent with the lack of the ceramide glycosyltransferases. Consistent with our previous study (Coetzee et al. 1996), TLC analysis revealed a slower moving band in the mutant samples that likely corresponds to the hydroxylated sphingomyelin species HFA-SPM (Fig 4C). We also compared the myelin lipids of *Cgt*$^{-/-}$ and wild-type mice by mass spectroscopy analysis. No substantial differences in sphingomyelin (SPM) were observed (6 nmol/mg in *Cgt*$^{-/-}$ and 5.4 nmol/mg in wild-type). The mass spectroscopy data indicated, however, that the loss of glycolipids in the mutants is compensated for by slightly increased cholesterol levels and about a 20% increase in phosphatidylethanolamine, phosphatidylserine and phosphatidylcholine. The mass spectrometric analysis also confirmed the increase in ceramide in the mutant animals.

Elimination of *Ugcg* function in Cgt$^{-/-}$ mice does not result in a more severe phenotype

At PND 12-16, mutant *Ugcg*$^{flox/flox}$;*Cnp/Cre;Cgt*$^{-/-}$ mice began to show an ataxic gait and head tremor, which were more pronounced during movement. A progressive weakness was also observed, culminating in hindquarter dragging at PND 18. Their survival range was between 16 and 24 days. Overall, these mutants were phenotypically indistinguishable from their *Cgt*$^{-/-}$ littermates.

Western blot analysis of the myelin-abundant protein MBP was performed using brain extracts from *Cgt*$^{-/-}$ and *Ugcg*$^{flox/flox}$;*Cnp/Cre;Cgt*$^{-/-}$ mice at PND 18. The quantitative analysis of MBP in the *Cgt*$^{-/-}$ and double mutant mice revealed no difference in the level of MBP among these genotypes, indicating that the elimination of oligodendroglial *Ugcg* expression on the *Cgt* deficient background does not affect myelin production (Fig. 5A).

Finally, morphometric analysis was performed on myelinated fibers of the cervical spinal cord ventral region of wild-type, *Cgt*$^{-/-}$, and *Ugcg*$^{flox/flox}$;*Cnp/Cre;Cgt*$^{-/-}$ mice. Both mutants showed higher G ratios and percentages of uncompacted myelin sheaths that were statistically significant when compared to wild-type. Nevertheless, no significant difference was observed between the two mutants (Table 1), indicating that the elimination of *Ugcg*, and therefore HFA-GlcCer, from *Cgt*$^{-/-}$ myelin does not result in increased abnormalities. Therefore, the presence of HFA-GlcCer in *Cgt*$^{-/-}$ myelin does not appear to play a compensatory role for the absence of galactolipids.

Discussion

In the present study we exploited a conditional *Ugcg* allele to examine the importance of GlcCer biosynthesis on oligodendroglial function. Though previous studies had assessed the effects of eliminating various ganglioside pathway enzymes, such as *Galgt1* and *Siat 9*, the importance of the *Ugcg* pathway in oligodendrocytes had remained undetermined. Although dysmyelination was a feature of these knockouts, axonal degeneration was also detected

(Sheikh et al. 1999; Yamashita et al. 2005b), leaving unclear the identity of the primary abnormality.

We conducted two sets of experiments to address the significance of the *Ugcg* pathway in oligodendrocytes. In the first study, we generated a line of mice with *Ugcg* selectively disrupted in oligodendrocytes. *Ugcg*$^{flox/flox}$*;Cnp/Cre* mice were not phenotypically or histologically distinguishable from their wild-type littermates, nor was their CNS ganglioside composition altered. This indicates that oligodendrocytes do not play a major role in ganglioside biosynthesis in the mouse brain. Moreover, the *Ugcg*$^{flox/flox}$*;Cnp/Cre* mutants did not show myelin or oligodendroglial abnormalities. Therefore, myelin changes seen in mice carrying mutant ganglioside biosynthesis genes (Jennemann et al. 2005; Sheikh et al. 1999; Yamashita et al. 2005b) are likely explained by altered neuronal ganglioside synthesis. Normal myelination requires trophic axon-to-oligodendrocyte signaling mediated by MAG and neuronal gangliosides, and complex gangliosides like GD1a and GT1b serve as MAG ligands, which may explain the myelin abnormalities in the ganglioside mutants (Quarles 2007; Vyas et al. 2002).

In the second part of our study, we exploited the *Ugcg*$^{flox/flox}$*;Cnp/Cre* mice to delete oligodendroglial *Ugcg* activity in *Cgt*$^{-/-}$ mice. *Cgt*$^{-/-}$ mice are not able to form GalCer or sulfatides, but are able to form compact myelin (Coetzee et al. 1996). In the absence of *Cgt*, HFA-ceramides are converted to HFA-GlcCer through the *Ugcg* pathway (Suzuki et al. 1999). The presence of HFA-GlcCer is interesting because it contains alpha hydroxyl fatty acids, which are normally found only in galactolipids. We have previously proposed that the accumulation of HFA-GlcCer in *Cgt*$^{-/-}$ myelin might have a compensatory effect in the absence of GalCer (Coetzee et al. 1996), allowing for the formation of compact myelin. This hypothesis is supported by the observation that GlcCer is detected in the myelin of primitive fish and crustacean species (Kishimoto 1986; Tamai et al. 1992).

The absence of HFA-GlcCer from total brain and myelin lipids isolated from *Ugcg*$^{flox/flox}$*;Cnp/Cre;Cgt*$^{-/-}$ mutant mice confirmed the efficiency of the Cnp/Cre recombination system in deleting the floxed *Ugcg* allele in oligodendrocytes. The *Ugcg*$^{flox/flox}$*;Cnp/Cre;Cgt*$^{-/-}$ mice were not distinguishable from their *Cgt*$^{-/-}$ littermates, having a similar body mass and life span of 16-24 days. Both the *Cgt*$^{-/-}$ and *Ugcg*$^{flox/flox}$*;Cnp/Cre;Cgt*$^{-/-}$ mutants displayed an ataxic gait and head tremor starting at PND 12-16. By PND 19-23, they showed weakness in their hindquarters. Morphometric analysis revealed that the myelin abnormalities displayed by the *Cgt*$^{-/-}$ mutant animals were not exacerbated by the absence of GluCer. Therefore, the accumulated HFA-GlcCer does not appear to have an ameliorating effect on the *Cgt*$^{-/-}$ phenotype.

In summary, mice lacking oligodendroglial *Ugcg* expression did not exhibit any phenotypic or myelin structural abnormalities. These experiments indicate the lack of functional significance of glucocerebroside-derived gangliosides, produced by oligodendrocytes, in myelin formation and stability. Furthermore, in contrast to expectations, these studies also demonstrated that the removal of oligodendroglial *Ugcg* expression in *Cgt*$^{-/-}$ mice did not have a deleterious effect on *Cgt*$^{-/-}$ myelin structure or phenotype. Although the myelin glycolipids normally represent approximately a third of the lipid content of myelin, these studies demonstrate that abundant and structurally intact myelin can form in their absence.

Acknowledgments

This work was supported by a grant from the National Institutes of Health (NS027336) to BP. Dr. Maria Traka was supported by a National Multiple Sclerosis Society postdoctoral fellowship award. Microscopy was performed at the VCU Department of Anatomy and Neurobiology Microscopy Facility, supported, in part, with funding from an NIH-NINDS Center core grant (5P30NS047463). Mass spectrometric analysis was performed at the Washington

University School of Medicine, supported in part, with funding from an NIA grant (NIA AG23168). We thank Dr. Darlene Douglas for critical comments on the manuscript, and Gloria Wright for help with the preparation of the figures. We would also like to thank Dr. Klaus-Armin Nave for generously providing us with the CNP/Cre mice.

References

Asou H, Mutou N, Hirano S. Localization of ganglioside GM1 on myelin, in dissociated cells from rat embryonic cerebral hemispheres, using biotinylated choleragen and avidin peroxidase. Neurosci Res. 1985; 2(5):399–406. [PubMed: 2993972]

Cheng H, Jiang X, Han X. Alterations in lipid homeostasis of mouse dorsal root ganglia induced by apolipoprotein E deficiency: a shotgun lipidomics study. J Neurochem. 2007; 101(1):57–76. [PubMed: 17241120]

Coetzee T, Fujita N, Dupree J, Shi R, Blight A, Suzuki K, Suzuki K, Popko B. Myelination in the absence of galactocerebroside and sulfatide: normal structure with abnormal function and regional instability. Cell. 1996; 86(2):209–19. [PubMed: 8706126]

Coetzee T, Suzuki K, Popko B. New perspectives on the function of myelin galactolipids. Trends Neurosci. 1998; 21(3):126–30. [PubMed: 9530920]

Dupree JL, Coetzee T, Blight A, Suzuki K, Popko B. Myelin galactolipids are essential for proper node of Ranvier formation in the CNS. J Neurosci. 1998; 18(5):1642–9. [PubMed: 9464989]

Eichberg J, Whittaker VP, Dawson RM. Distribution of lipids in subcellular particles of guinea-pig brain. Biochem J. 1964; 92(1):91–100. [PubMed: 5840391]

Han X, Gross RW. Shotgun lipidomics: electrospray ionization mass spectrometric analysis and quantitation of cellular lipidomes directly from crude extracts of biological samples. Mass Spectrom Rev. 2005; 24(3):367–412. [PubMed: 15389848]

Han X, Yang K, Gross RW. Microfluidics-based electrospray ionization enhances the intrasource separation of lipid classes and extends identification of individual molecular species through multi-dimensional mass spectrometry: development of an automated high-throughput platform for shotgun lipidomics. Rapid Commun Mass Spectrom. 2008; 22(13):2115–24. [PubMed: 18523984]

Ichikawa S, Sakiyama H, Suzuki G, Hidari KI, Hirabayashi Y. Expression cloning of a cDNA for human ceramide glucosyltransferase that catalyzes the first glycosylation step of glycosphingolipid synthesis. Proc Natl Acad Sci U S A. 1996; 93(22):12654. [PubMed: 8901638]

Jennemann R, Sandhoff R, Wang S, Kiss E, Gretz N, Zuliani C, Martin-Villalba A, Jager R, Schorle H, Kenzelmann M. Cell-specific deletion of glucosylceramide synthase in brain leads to severe neural defects after birth. Proc Natl Acad Sci U S A. 2005; 102(35):12459–64. others. [PubMed: 16109770]

Kilkus J, Goswami R, Testai FD, Dawson G. Ceramide in rafts (detergent-insoluble fraction) mediates cell death in neurotumor cell lines. J Neurosci Res. 2003; 72(1):65–75. [PubMed: 12645080]

Kishimoto Y. Phylogenetic development of myelin glycosphingolipids. Chem Phys Lipids. 1986; 42(1-3):117–28. [PubMed: 3549016]

Kolter T, Proia RL, Sandhoff K. Combinatorial ganglioside biosynthesis. J Biol Chem. 2002; 277(29): 25859–62. [PubMed: 12011101]

Kotani M, Kawashima I, Ozawa H, Terashima T, Tai T. Differential distribution of major gangliosides in rat central nervous system detected by specific monoclonal antibodies. Glycobiology. 1993; 3(2):137–46. [PubMed: 8490240]

Lappe-Siefke C, Goebbels S, Gravel M, Nicksch E, Lee J, Braun PE, Griffiths IR, Nave KA. Disruption of Cnp1 uncouples oligodendroglial functions in axonal support and myelination. Nat Genet. 2003; 33(3):366–74. [PubMed: 12590258]

Ledeen RW, Yu RK, Eng LF. Gangliosides of human myelin: sialosylgalactosylceramide (G7) as a major component. J Neurochem. 1973; 21(4):829–39. [PubMed: 4754859]

Loeb JA, Dawson G. Reversible exchange of glycosphingolipids between human high and low density lipoproteins. J Biol Chem. 1982; 257(20):11982–7. [PubMed: 7118925]

Morell P, Radin NS. Synthesis of cerebroside by brain from uridine diphosphate galactose and ceramide containing hydroxy fatty acid. Biochemistry. 1969; 8(2):506–12. [PubMed: 5793706]

Norton WT, Poduslo SE. Myelination in rat brain: method of myelin isolation. J Neurochem. 1973; 21(4):749–57. [PubMed: 4271082]

Quarles RH. Myelin-associated glycoprotein (MAG): past, present and beyond. J Neurochem. 2007; 100(6):1431–48. [PubMed: 17241126]

Schulte S, Stoffel W. Ceramide UDPgalactosyltransferase from myelinating rat brain: purification, cloning, and expression. Proc Natl Acad Sci U S A. 1993; 90(21):10265–9. [PubMed: 7694285]

Senn HJ, Orth M, Fitzke E, Wieland H, Gerok W. Gangliosides in normal human serum. Concentration, pattern and transport by lipoproteins. Eur J Biochem. 1989; 181(3):657–62. [PubMed: 2731542]

Sheikh KA, Sun J, Liu Y, Kawai H, Crawford TO, Proia RL, Griffin JW, Schnaar RL. Mice lacking complex gangliosides develop Wallerian degeneration and myelination defects. Proc Natl Acad Sci U S A. 1999; 96(13):7532–7. [PubMed: 10377449]

Shen BW, Kwok BC, Dawson G. Glycosphingolipid-high density lipoprotein 3 interactions. II. Characterization of the glycosphingolipid component of modified high density lipoprotein. J Biol Chem. 1981; 256(18):9705–10. [PubMed: 7287704]

Stahl N, Jurevics H, Morell P, Suzuki K, Popko B. Isolation, characterization, and expression of cDNA clones that encode rat UDP-galactose: ceramide galactosyltransferase. J Neurosci Res. 1994; 38(2):234–42. [PubMed: 7521399]

Suzuki K. Formation and turnover of myelin ganglioside. J Neurochem. 1970; 17(2):209–13. [PubMed: 5494050]

Suzuki K, Poduslo JF, Poduslo SE. Further evidence for a specific ganglioside fraction closely associated with myelin. Biochim Biophys Acta. 1968; 152(3):576–86. [PubMed: 4873454]

Suzuki K, Poduslo SE, Norton WT. Gangliosides in the myelin fraction of developing rats. Biochim Biophys Acta. 1967; 144(2):375–81. [PubMed: 6064614]

Suzuki K, Vanier MT, Coetzee T, Popko B. Drastically abnormal gluco- and galactosylceramide composition does not affect ganglioside metabolism in the brain of mice deficient in galactosylceramide synthase. Neurochem Res. 1999; 24(4):471–4. [PubMed: 10227678]

Tamai Y, Kojima H, Saito S, Takayama-Abe K, Horichi H. Characteristic distribution of glycolipids in gadoid fish nerve tissues and its bearing on phylogeny. J Lipid Res. 1992; 33(9):1351–9. [PubMed: 1402402]

Ueno K, Ando S, Yu RK. Gangliosides of human, cat, and rabbit spinal cords and cord myelin. J Lipid Res. 1978; 19(7):863–71. [PubMed: 712245]

Vyas AA, Patel HV, Fromholt SE, Heffer-Lauc M, Vyas KA, Dang J, Schachner M, Schnaar RL. Gangliosides are functional nerve cell ligands for myelin-associated glycoprotein (MAG), an inhibitor of nerve regeneration. Proc Natl Acad Sci U S A. 2002; 99(12):8412–7. [PubMed: 12060784]

Wiesner DA, Kilkus JP, Gottschalk AR, Quintans J, Dawson G. Anti-immunoglobulin-induced apoptosis in WEHI 231 cells involves the slow formation of ceramide from sphingomyelin and is blocked by bcl-XL. J Biol Chem. 1997; 272(15):9868–76. [PubMed: 9092523]

Yamashita T, Allende ML, Kalkofen DN, Werth N, Sandhoff K, Proia RL. Conditional LoxP-flanked glucosylceramide synthase allele controlling glycosphingolipid synthesis. Genesis. 2005a; 43(4): 175–80. [PubMed: 16283624]

Yamashita T, Wada R, Sasaki T, Deng C, Bierfreund U, Sandhoff K, Proia RL. A vital role for glycosphingolipid synthesis during development and differentiation. Proc Natl Acad Sci U S A. 1999; 96(16):9142–7. [PubMed: 10430909]

Yamashita T, Wu YP, Sandhoff R, Werth N, Mizukami H, Ellis JM, Dupree JL, Geyer R, Sandhoff K, Proia RL. Interruption of ganglioside synthesis produces central nervous system degeneration and altered axon-glial interactions. Proc Natl Acad Sci U S A. 2005b; 102(8):2725–30. [PubMed: 15710896]

Yang K, Cheng H, Gross RW, Han X. Automated lipid identification and quantification by multidimensional mass spectrometry-based shotgun lipidomics. Anal Chem. 2009; 81(11):4356–68. [PubMed: 19408941]

Zimmerman L, Parr B, Lendahl U, Cunningham M, McKay R, Gavin B, Mann J, Vassileva G, McMahon A. Independent regulatory elements in the nestin gene direct transgene expression to neural stem cells or muscle precursors. Neuron. 1994; 12(1):11–24. [PubMed: 8292356]

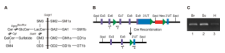

Figure 1. Ganglioside pathway and recombination analysis of the floxed *Ugcg* allele in *Ugcg*$^{flox/flox}$;*Cnp/Cre* mice

(A) Simultaneous global disruption of *Cgt* and deletion of *Ugcg* in oligodendrocytes results in the absence of GlcCer- and GalCer-based GSLs in CNS myelin. Double lines show the blockage in biosynthetic pathways of *Cgt*, *Ugcg*, *Siat9* and *Galtg1* mice. (B) Crossing *Ugcg*$^{flox/flox}$ mice with Cnp/Cre mice leads to the excision of the *Ugcg* gene in double mutants; the green triangles represent lox P sites. (C) The recombined floxed *Ugcg* allele was readily detected by PCR of genomic DNA extracted from *Ugcg*$^{flox/flox}$;*Cnp/Cre* brain and spinal cord (lanes 1 and 2, respectively) but barely detected in heart (lane 3) using primers 1 and 3, which yield a 250 bp fragment. The black arrows designate the primer locations.

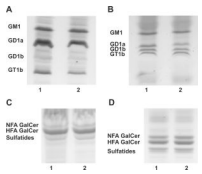

Figure 2. Deletion of *Ugcg* in oligodendrocytes does not affect the ganglioside profile of PND 18 *Ugcg*$^{flox/flox}$;*Cnp/Cre* brains

(A) The predominant brain gangliosides, GM1, GD1a, GD1b, and GT1b, were detected in the total brain lipid extracts of wild-type (lane1) and *Ugcg*$^{flox/flox}$;*Cnp/Cre* mice (lane 2). (B) The same pattern of gangliosides was observed in myelin lipid extracts of wild-type (lane 1) and mutant brains (lane 2). (C) The neutral lipid fraction was isolated from brains of wild-type (lane1) and *Ugcg*$^{flox/flox}$;*Cnp/Cre* mice (lane 2). HFA-GalCer, NFA-containing GalCer, and sulfatides were detected in both mutant and wild-type mice. (D) The presence of HFA-GalCer, NFA-GalCer, and sulfatides was also observed in the myelin of wild-type (lane 1) and *Ugcg*$^{flox/flox}$;*Cnp/Cre* mice (lane 2).

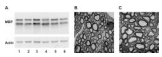

Figure 3. PND18 *Ugcg*$^{flox/flox}$*;Cnp/Cre* mutants demonstrate similar MBP expression and histological features as wild-type littermates

(A) MBP levels in brain extracts of wild-type (lanes 1-3) and *Ugcg*$^{flox/flox}$ (lanes 4-6) mice are similar. EM analysis of myelinated fibers in the ventral white matter of the cervical spinal cord showed no difference in myelination between *Ugcg*$^{flox/flox}$*;Cnp/Cre* mice (B) and wild-type littermates (C). Bar: 2 μm.

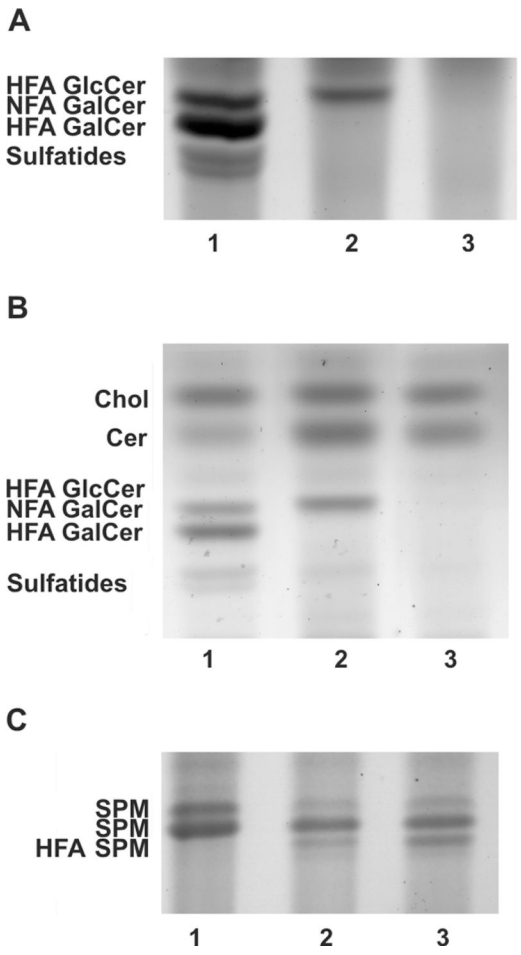

Figure 4. HFA-GlcCer is completely eliminated in *Ugcg*$^{flox/flox}$;*Cnp/Cre;Cgt*$^{-/-}$ mice

(A) HFA-GalCer, NFA-containing GalCer, and sulfatides were detected in total brain lipid extracts of wild-type mice (lane 1) and were absent in *Cgt*$^{-/-}$ mice; however, an HFA-GlcCer lipid band was detected in *Cgt*$^{-/-}$ mice (lane 2). HFA-GlcCer was completely eliminated in *Ugcg*$^{flox/flox}$;*Cnp/Cre;Cgt*$^{-/-}$ mice (lane 3), indicating that the Cre recombinase efficiently excises the floxed *Ugcg* allele in oligodendrocytes. (B) The lipid band patterns detected in myelin lipid extracts from wild-type (lane 1), *Cgt*$^{-/-}$ (lane 2), and *Ugcg*$^{flox/flox}$;*Cnp/Cre;Cgt*$^{-/-}$ (lane 3) mouse brains also confirmed the absence of HFA-GlcCer and an increased level of ceramide in the *Cgt*$^{-/-}$ and *Ugcg*$^{flox/flox}$;*Cnp/Cre;Cgt*$^{-/-}$ mice. (C) The detection of a slower mobility band in *Cgt*$^{-/-}$ and *Ugcg*$^{flox/flox}$;*Cnp/Cre;Cgt*$^{-/-}$ mice is likely indicative of HFA-SFM.

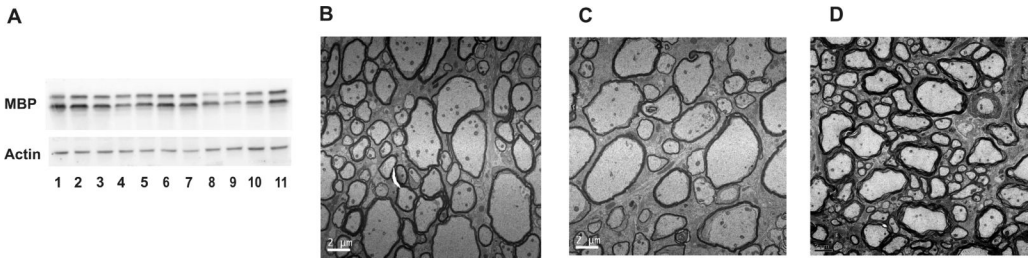

Figure 5. The *Ugcg*$^{flox/flox}$*;Cnp/Cre;Cgt*$^{-/-}$ mice have similar MBP expression and histological characteristics as compared to *Cgt*$^{-/-}$ mice

(A) MBP levels in the brain are not significantly different among the wild-type (lanes 1-3), *Cgt*$^{-/-}$ (lanes 4-7), and *Ugcg*$^{flox/flox}$*;Cnp/Cre;Cgt*$^{-/-}$ (lanes 8-11) mice at PND 18. EM analysis of myelinated fibers in the ventral white matter of the cervical spinal cord showed no significant difference in myelination between *Cgt*$^{-/-}$ (B) and *Ugcg*$^{flox/flox}$*;Cnp/Cre;Cgt*$^{-/-}$ (C) mice. Both mutants had a thinner myelination as compared to age-matched controls at PND 18 (D). Bar: 2 μm.

Table 1

Morphometric Analysis of Myelination at PND 18

Genotype	G ratio	% Uncompacted Myelin
Wt	0.79 $^{+}/-$ 0.06	3.2 $^{+}/-$ 1.3
Ugcg$^{flox/flox}$;Cnp/Cre	0.81 $^{+}/-$ 0.06	3.3 $^{+}/-$ 1.4
Cgt $-/-$	0.86 $^{+}/-$ 0.05	7.2 $^{+}/-$ 1.3
Ugcg$^{flox/flox}$;Cnp/Cre;Cgt$^{-/-}$	0.87 $^{+}/-$ 0.05	8.3 $^{+}/-$ 4.2

Morphometric analysis of myelinated fibers of ventral spinal cord from wild-type and mutant animals: Difference of G ratios (middle column) and percentile of uncompacted myelin (right column) were not significant either between the *Wt* and *Ugcg$^{flox/flox}$;Cnp/Cre* or between *Cgt* $-/-$ and *Ugcg$^{flox/flox}$;Cnp/Cre;Cgt*.